global lightning activity will increase substantially in a warmer climate.

REFERENCES AND NOTES

1. J. K. Angell, *Mon. Weather Rev.* **114**, 1922 (1986).
2. P. D. Jones *et al.*, *Nature* **322**, 430 (1986).
3. J. Hansen and S. Lebedeff, *J. Geophys. Res.* **92**, 13345 (1987).
4. E. R. Williams, *ibid.* **90**, 6013 (1985).
5. R. E. Orville and R. W. Henderson, *Mon. Weather Rev.* **114**, 2640 (1986).
6. M. Kotaki, I. Kuriki, C. Katoh, H. Sugiuchi, *J. Radio Res. Lab. (Tokyo)* **28**, 49 (1981).
7. The lightning counts were obtained with a CGR3-type lightning detector (*8*) and are archived by the Australian Bureau of Meteorology.
8. D. Mackerras, *J. Geophys. Res.* **90**, 6195 (1985).
9. The lightning counts were obtained with a SAFIR interferometer system (P. Richard, personal communication).
10. F. de la Rosa, personal communication.
11. R. de Araujo, personal communication.
12. R. Jayaratne, personal communication.
13. R. Orville, personal communication; these counts were for ground flashes identified with Lightning Location and Protection (LLP) equipment.
14. E. R. Williams and N. Renno, *Mon. Weather Rev.*, in press.
15. S. A. Rutledge, E. R. Williams, T. D. Keenan, *Bull. Am. Meteorol. Soc.* **73**, 3 (1992).
16. E. R. Williams *et al.*, *J. Atmos. Sci.*, in press.
17. F. J. W. Whipple, *Q. J. R. Meteorol. Soc.* **55**, 1 (1929).
18. W. O. Schumann, *Z. Naturforsch. Teil A* **7**, 149 (1952).
19. P. V. Bliokh, A. P. Nikolaenko, Yu. F. Filippov, *Schumann Resonances in the Earth-Ionosphere Cavity* (Perigrinus, London, 1980).
20. C. Polk, in *CRC Handbook of Atmospherics*, H. Volland, Ed. (CRC Press, Boca Raton, FL, 1982), vol. 1, p. 112.
21. M. Balser and C. A. Wagner, *J. Geophys. Res.* **67**, 619 (1962).
22. T. R. Madden and W. Thompson, *Rev. Geophys.* **3**, 211 (1965).
23. R. Gendrin and R. Stefant, in *Propagation of Radio Waves at Frequencies Below 30 kc/s*, W. T. Blackband, Ed. (Pergamon, New York, 1964), p. 371.
24. T. Ogawa, Y. Tanaka, M. Yasuhara, *J. Geomagn. Geoelec.* **21**, 447 (1969).
25. M. Clayton and C. Polk, in *Electrical Processes in Atmospheres*, H. Dolezalek and R. Reiter, Eds. (Steinkopff, Darmstadt, 1977), pp. 440–449.
26. D. D. Sentman and B. J. Fraser, *J. Geophys. Res.* **96**, 15973 (1991).
27. C. Polk, *Geophysics and Space Data Bulletin* [Space Physics Laboratory, Air Force Cambridge Research Laboratories, Hanscom Air Force Base, MA (1967–1974)].
28. A. H. Oort, *NOAA (Natl. Oceanic Atmos. Adm.) Prof. Pap 14* (April 1983).
29. R. E. Orville and D. W. Spencer, *Mon. Weather Rev.* **107**, 934 (1979).
30. R. Markson, *Nature* **320**, 588 (1986).
31. E. R. Williams and S. J. Heckman, *J. Geophys. Res.*, in press.
32. R. P. Muhleisen, *Pure Appl. Geophys.* **84**, 112 (1971).
33. R. Markson, *J. Geophys. Res.* **90**, 5967 (1985).
34. _____, personal communication.
35. E. R. Williams, *J. Geophys. Res.* **94**, 13151 (1989).

36. Long-standing discussions with T. Madden, R. Markson, C. Polk, and D. Sentman on SR and V_t have been very valuable. C. Polk of the University of Rhode Island at Kingston provided vital access to the SR data set. R. Markson provided his Bahamas data set for comparisons. I thank S. Heckman, N. Renno, D. Boccippio, and E. Rasmussen, who performed analyses of electrical data sets and tropical soundings. H. Wilson of the National Aeronautics and Space Administration Goddard Institute for Space Studies provided the tropical temperature anomalies. The lightning–wet-bulb relations at low latitudes were established through the assistance of A. Aka, A. Bhattacharya, I. Butterworth, J. Core, R. de Araujo, F. de la Rosa, M. Ianoz, R. Jayaratne, A. Liew, D. Mackerras, R. Orville, P. Richard, and H. Torres. Ongoing studies of tropical lightning in DUNDEE (Down Under Doppler and Electrical Experiment) have been supported by the Physical Meteorology section of the National Science Foundation under grant ATM-8818695 with the assistance of R. Taylor.

24 February 1992; accepted 26 March 1992

An Intercomparison of Tropospheric OH Measurements at Fritz Peak Observatory, Colorado

George H. Mount and Fred L. Eisele

The hydroxyl radical (OH) controls the lifetimes and therefore the concentrations of many important chemical species in Earth's lower atmosphere including several greenhouse and ozone-depleting species. Two completely different measurement techniques were used in an informal intercomparison to determine tropospheric OH concentrations at Fritz Peak Observatory, Colorado, from 15 July to 24 August 1991. One technique determined OH concentrations by chemical analysis; the other used spectroscopic absorption on a long path. The intercomparison showed that ambient OH concentrations can now be measured with sufficient sensitivity to provide a test for photochemical models, with the derived OH concentrations agreeing well under both polluted and clean atmospheric conditions. Concentrations of OH on all days were significantly lower than model predictions, perhaps indicating the presence of an unknown scavenger. The change in OH concentration from early morning to noon on a clear day was found to be only a factor of 2.

The determination of OH concentration is fundamental to an understanding of atmospheric chemistry, but its measurement has been fraught with difficulties. Because OH noontime concentrations are thought to be extremely low [approximately 0.1 part per trillion by volume (pptv)], measurement is difficult. Initial measurements in the troposphere were based on laser-induced fluorescence of OH rotational lines in the ultraviolet (UV) part of the spectrum (*1*, *2*), but many problems were discovered (*3*, *4*). Modifications have been marginally successful (*5*), but not to the levels necessary to test photochemical theories (*6*). Long-path absorption of laser light in the UV has been used to measure OH concentrations near Julich, Germany (*7–9*). Although this region is industrially polluted, OH levels were measured reliably to several $\times 10^6$ mol/cm^3. Real-time chemical tracer techniques have been used without notable success; however, global tracer techniques have shown some success. Summaries of the reactions and rate constants used for theoretical calculation of tropospheric OH chemistry are given in (*10*, *11*). To date, the theory is far more advanced than the measurements. In this paper we describe an intercomparison of measurements of tropospheric OH by two highly sensitive instruments operating simultaneously.

The first technique (*12*) is an in situ ion-assisted measurement with a lower sensitivity limit of 1×10^5 mol/cm^3 in short time integrations (minutes). The calibration is difficult and dependent on chemical interpretation. The second technique (*13*) is a laser-based long-path absorption experiment with a sensitivity limit of $\sim 4 \times 10^5$ mol/cm^3, also with a time resolution of minutes. This instrument has a simple absolute calibration, but determination of the OH concentration is dependent on determination of the local spectral continuum, which is difficult to measure because of spectral interferences from other atmospheric trace species.

The Georgia Tech (GT) ion-assisted measurement of OH is performed by sampling air through a turbulence-reducing scoop and down a flow tube–reactor at a velocity of 0.6 m/s. The OH present in the center of the flow tube is titrated into $H_2{}^{34}SO_4$ by the addition of $^{34}SO_2$. The SO_2 converts OH into HSO_3, which reacts with O_2 and then H_2O to form H_2SO_4. Mixing is accomplished by the continuous injection of an SO_2-N_2 mixture perpendicular to the sampled air flow through two opposed needles. The injected mixture makes up less than 1% of the sample flow and causes turbulence primarily in the center of the flow tube. There is little to no mixing or turbulence at the walls. Because only species in the center of the flow are sampled, the lack of mixing at the walls is of little concern. To ensure that all of the OH in the sampled air has been converted

G. H. Mount, Aeronomy Laboratory, Environmental Research Laboratories, National Oceanic and Atmospheric Administration, 325 Broadway, Boulder, CO 80303.
F. L. Eisele, Physical Sciences Laboratory, Georgia Tech Research Institute, Georgia Institute of Technology, Atlanta, GA 30332.

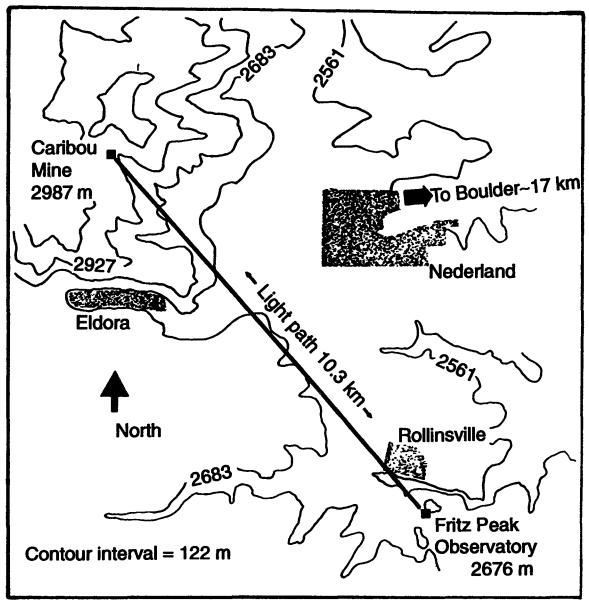

Fig. 1. Topography of the region between Fritz Peak Observatory and Caribou, Colorado, where the AL retroreflector and the GT experiment were located. Average beam height for the AL laser beam was several hundred meters above the ground. For normal westerly wind, the beam crosses upwind of the only sizable town (Nederland, population 300). Populated areas are indicated by shaded areas on the map.

into H_2SO_4, SO_2 is added until the H_2SO_4 concentration is independent of the amount of SO_2 added. The SO_2 concentration is then typically maintained at about twice that level.

The concentration of $H_2{}^{34}SO_4$ formed from the titration of OH is then measured with a chemical ionization method. In an isolated high-pressure source NO_3^- ions are prepared and forced by electric fields into the titrated air sample. They then react with H_2SO_4 to form HSO_4^- ions, and the resulting HSO_4^-/NO_3^- core ion ratio is used to calculate the $H_2{}^{34}SO_4$ concentration.

Ion concentrations are measured with a differentially pumped quadrupole mass spectrometer. All reactions are carried out in laminar gas flow at atmospheric pressure in an effectively wall-less reactor. The OH titration is accomplished in ~10 to 20 ms, and the total transit time for the OH-air sample from the inlet to the analysis region is less than 1 s.

Air is sampled continuously from ~3 m above the ground, and an integration time of ~20 s is required for each OH measurement. With the present apparatus a 5-min integration time results in a detection sensitivity of $\sim 1 \times 10^5$ mol/cm^3. The total estimated uncertainty associated with the ion-assisted sampling and measurement technique is $\pm 60\% \pm 1 \times 10^5$ mol/cm^3. All GT data are shown as 5-min averages.

The Aeronomy Laboratory (AL) instrumentation measures the spectral line profiles of individual OH molecular rotational lines in the A-X electronic transition absorbed in the near-UV over a long path (*13*). This is a particularly clean method of determining OH concentration. It depends only on well-measured spectroscopic parameters determined from laboratory experiments with good accuracy (10%), physical variables (such as light path length) that are easily and accurately determined, and the measured fractional spectral absorption. The experimental apparatus consists of six basic components: (i) a spectrally bright and broad (tens of millijoules per pulse over several tenths of nanometers) UV XeCl excimer laser light source with optics for directing a low-divergence, expanded light beam into ambient air outside of the observatory; (ii) a 1-m^2 121-element retroreflector mirror system located 10.3 km away to collect the laser light beam and return it to the observatory for a total absorption path length of 20.6 km; (iii) a telescope collector located in the laboratory at the observatory; (iv) a high-resolution (resolving power > 500,000) dual-channel spectrograph to allow accurate measurement of atmospheric absorption of individual rotational lines in the UV electronic OH bands near 308 nm; (v) a two-channel array detector system with signal-to-noise ratio greater than 10^4 per integration that allows simultaneous observation of both laser and atmospheric absorbed laser light at all wavelengths in a spectral interval sufficient to include measurement of several OH rotational lines simultaneously; and (vi) a data collector and analysis system that allows computer control of the hardware.

Laser light exits the laser to a beam splitter, which sends part of the laser light directly into the spectrograph (channel 1); the transmitted light is directed to a beam expander and then travels 20.6 km to the retroreflector array and back to the observatory, where it is collected by a Cassegrain telescope and sent into the spectrograph (channel 2). The ratio of these two signals gives the atmospheric absorption signature. This ratio is then used in Beer's law to determine the concentration of OH. All AL data are shown as 15-min averages. Absolute measurement errors for the laser long-path technique are ±50% below 2×10^6 mol/cm^3 and ±30% above that. In addition to the system for determination of OH abundance, a completely independent instrument at the observatory measured simultaneously on the long path the concentration of O_3, water vapor, NO_2, NO_3, SO_2, formaldehyde, and other trace gas species that affect the concentration of OH.

Measurements were made using these two instruments at the AL's Fritz Peak Observatory near Rollinsville, Colorado, approximately 40 km west of the edge of the Great Plains and 3 km east of the continental divide at an altitude of 2700 m (Fig. 1). The Caribou site where the in situ measurements were performed is 10.3 km distant and at an elevation of about 3000 m. The laser beam path is a few hundred meters above the tree line. The wind is generally from the west; therefore, the air is usually quite clean (the nearest large pollution source is Salt Lake City, ~600 km away). Local sources of pollution are small. During the summer months, however, easterly upslope winds often bring pollution from the Denver metropolitan area to the region of the observatory. Several such events occurred during the intercomparison. The intercomparison was informal and not blind; discussion occurred between the investigators as measurements were made.

Temperature, wind speed, wind direction, humidity, solar flux, and other meteorological parameters of interest were measured at both ends of the laser path. Also stationed at Caribou was a set of GT instruments that measured CO, SO_2, gaseous H_2SO_4, and aerosol number and size distribution together with AL instrumentation (*14*) that measured O_3, SO_2, NO, NO_2, NO_y, solar UV flux, and other trace gases of interest that can affect the OH measurements.

The instruments did not operate every day of the 5-week period. Approximately 7 days of high-quality overlapped data were obtained. Here we discuss only two fairly typical days: 23 August, which experienced polluted conditions, and 24 August, which experienced clean and clear conditions until early afternoon.

Agreement between the two OH measurement techniques was quite good for most of 23 August (Fig. 2A). The major discrepancy was that at ~1300 MST clouds reached the Caribou site and reduced the OH concentration locally. Intermittent periods of cloud cover were common on 23 August (Fig. 2B). Minima in solar irradiance and relatively low OH concentrations occurred before 0815 hours, between 0945 and 1045 hours, and after 1245 hours. Long-path OH concentrations also varied with solar flux, but the average flux over the

path length was more difficult to quantify.

Concentrations of OH measured throughout the intercomparison typically increased in more polluted air masses. Increased SO_2 concentrations are a good indicator of this polluted air as are high NO_x, NO_y, CO, and aerosol concentrations. Concentrations of SO_2 were enhanced after 1100 hours on 23 August (Fig. 2C) and correspond well with increased OH concentrations measured at the Caribou site during the same period. Long-path absorption measurements of SO_2 and NO_2 are not available for 23 or 24 August.

Agreement in deduced OH concentration between the two techniques (Fig. 3A) was quite good on 24 August, the clearest day on which intercomparative measurements were made. Aerosol and NO_x data again suggest an influx of polluted air at about 1330 hours at the Caribou site, at which time clouds also began to block the solar flux. Winds were strong and from the west (clean) until 1330 hours, when the wind shifted to the east (Fig. 3B). Although there are not good UV solar flux data for the Caribou site that day, and no SO_2, CO, or aerosol data between 1430 and 1645 hours, visible solar flux data taken at Fritz Peak show a perfectly clear sky until about 1330 hours. Rain occurred on the long path after 1400 hours.

The data from both days show that fluctuations in OH concentration typically correspond to fluctuations in solar flux or changing air masses (pollution episodes). These atmospheric conditions can be quite different between the long-path and the GT in situ site. Conversely, as can be seen from earlier measurements, stable uniform solar flux and air masses lead to smoothly varying OH concentrations (*12*). Because intermittent cloudiness was common on most afternoons, it is not surprising that the data sets have considerable scatter. Solar flux and air mass variations did not, however, occur simultaneously over the absorption path; thus, observed short-term changes in OH concentration are likely real but difficult to compare between the in situ and long-path techniques.

On 24 August, the absolute values of the OH concentration were extremely low, never higher than ~2 × 10^6 mol/cm^3 before the pollution episode, which began shortly after noon. The change in OH is particularly small in the morning; OH concentrations increased only a factor of about 2 from early morning to early afternoon. The steeper increase experienced after noon was presumably caused by pollution, which accompanied the wind shift evident in Fig. 3B. On 23 August, the morning values did not increase by much until after 1100 hours when they went up significantly, also presumably because of pollution. On other polluted days OH concentrations were as high as 8 × 10^6 mol/cm^3 and increased sharply in the morning as the solar UV flux increased.

This intercomparison of two different tropospheric OH measurement techniques suggests that ambient OH concentrations can now be measured with sufficient sensitivity to test photochemical models. The measured OH concentrations compared surprisingly well in both clean and polluted air masses throughout the measurement period with few exceptions. The exceptions, when they did occur, still represent agreement within a factor of 2 or 3 and could usually be explained by differences in air masses measured (pollution episodes) or solar flux levels experienced at the two sites. Nearly always the long-path measurements were higher than the in situ measurements. Models suggest higher OH concentrations than those seen by either experimental technique (*15*); the discrepancies between measurements and model calculations on most days appear to be much greater than differences between the measurements and considerably exceeded the errors of measurement. Perhaps this can be understood in terms of the presence of an unknown hydrocarbon scavenger. Thus, despite the instrumental uncertainties and the differences in sampled air masses, this favorable intercomparison indicates a significant advance in the ability to measure tropospheric OH concentrations at very low levels. The ancillary trace gas measurements made during the intercomparison give hope that the chemistry can be understood.

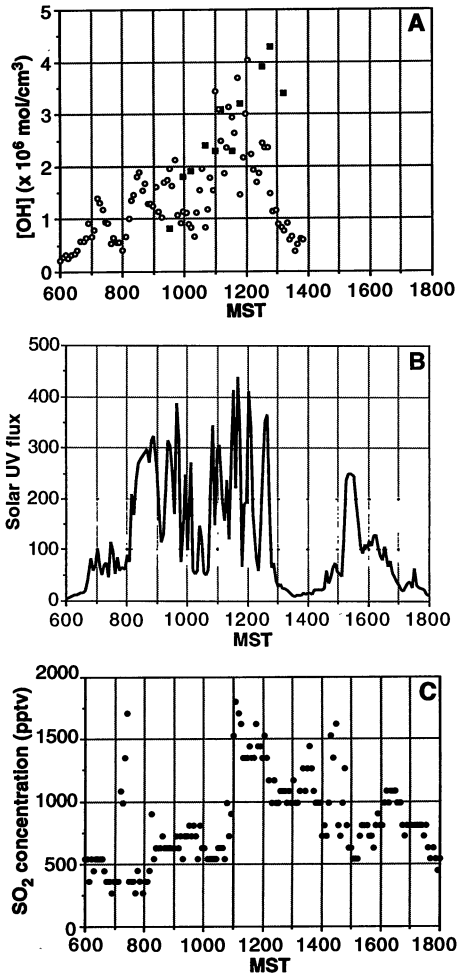

Fig. 2. (**A**) Hydroxyl concentration from both experiments on 23 August 1991 (GT, circles; AL, squares). This day was partly cloudy and fairly polluted, especially in the afternoon, with air from the Denver metropolitan area. (**B**) UV solar flux measured at the Caribou site by GT on 23 August. (**C**) Sulfur dioxide concentration measured at the Caribou site by GT on 23 August.

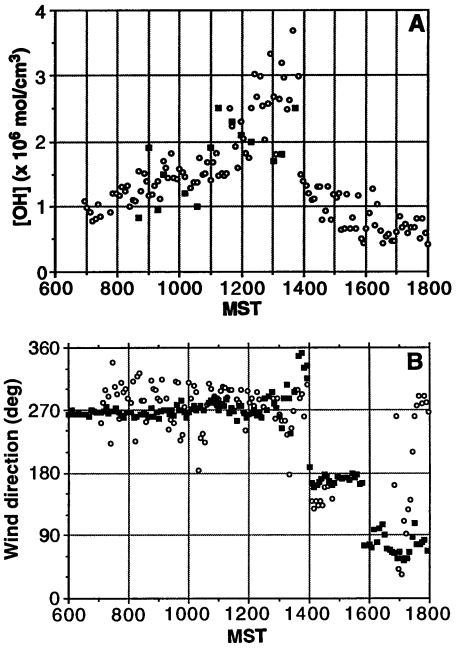

Fig. 3. (**A**) Hydroxyl concentration measured from both experiments on 24 August 1991 (GT, circles; AL, squares). This day was completely free of clouds and experienced undetectable levels of pollution until early afternoon. Rain occurred on the long path after about 1400 hours. (**B**) Wind direction as measured at the Caribou site (circles) and Fritz Peak (squares) on 24 August. The clear westerly flow is characteristic of very clean conditions.

REFERENCES AND NOTES

1. D. Davis, W. Heaps, T. McGee, *Geophys. Res. Lett.* **3**, 331 (1976).
2. C. Wang, L. I. Davis, C. H. Wu, S. Japar, *Appl. Phys. Lett.* **28**, 14 (1976).
3. G. Ortgies, K. Gericke, F. Comes, *Geophys. Res. Lett.* **7**, 905 (1980).
4. D. Davis *et al.*, *ibid.* **8**, 73 (1981).
5. T. M. Hard, C. Y. Chan, A. A. Mehrabzadeh, W. H. Pan, R. J. O'Brien, *Nature* **322**, 617 (1986).
6. G. Smith and D. Crosley, *J. Geophys. Res.* **95**, 16427 (1990).
7. G. Hubler *et al.*, *ibid.* **89**, 1309 (1984).
8. U. Platt *et al.*, *ibid.* **93**, 5159 (1988).
9. A. Hofzumahaus, H.-P. Dorn, J. Callies, U. Platt, D. Ehhalt, *Atmos. Environ. Part A* **25**, 2017 (1991).
10. J. Logan, M. Prather, S. Wofsy, M. McElroy, *J. Geophys. Res.* **86**, 7210 (1981).
11. D. Perner *et al.*, *J. Atmos. Chem.* **5**, 185 (1987).

12. F. L. Eisele and D. J. Tanner, *J. Geophys. Res.* **96**, 9295 (1991).
13. G. Mount, *ibid.* **97**, 2427 (1992).
14. D. Parrish *et al.*, *ibid.* **95**, 1817 (1990).
15. M. Trainer *et al.*, *ibid.* **92**, 11879 (1987).
16. We thank D. Tanner, E. Marovich, and I. Leifer for help during the intercomparison. T. Hendricks of the Hendricks Mining Company provided the site for the instrumentation located at Caribou, CO. The GT experiment was funded by Office of Exploratory Research, U.S. Environmental Protection Agency, contract R817121, and National Science Foundation grant ATM 9021522, and the AL experiment was funded by the National Oceanic and Atmospheric Administration Radiatively Important Trace Species Program.

13 January 1992; accepted 13 March 1992

Synthesis and Electronic Transport of Single Crystal K_3C_{60}

X.-D. Xiang, J. G. Hou, G. Briceño, W. A. Vareka, R. Mostovoy, A. Zettl,* Vincent H. Crespi, Marvin L. Cohen

Sizable single crystals of C_{60} have been synthesized and doped with potassium. Above the superconducting transition temperature T_c, the electrical resistivity $\rho(T)$ displays a classic metal-like temperature dependence. The transition to the superconducting state at $T_c = 19.8$ K is extremely sharp, with a transition width $\Delta T < 200$ mK. In contrast to transport behavior of doped polycrystalline and granular thin films, no anomalous fluctuations are observed near T_c in single crystal specimens.

The discovery of superconductivity in heavy alkali metal–doped C_{60} (*1*) has generated great theoretical and experimental interest. Although many experimental results of doped fullerenes have begun to shed some light on the underlying physics of these unique materials, nearly all previous measurements have been performed on weakly linked polycrystalline (*2*) or granular thin films samples (*3*). Reliable measurements on single crystals are essential for establishing intrinsic properties and determining the superconductivity mechanism.

We report here the synthesis and electronic transport measurements of high-quality single crystals of K_3C_{60}. Measurements of the dc electrical resistivity $\rho(T)$ show an intrinsic metal-like temperature dependence below room temperature, with an extremely sharp transition to the superconducting ground state at $T_c = 19.8$ K; no evidence is found for strong fluctuation effects near T_c. These results are in sharp contrast to the behavior of polycrystalline and thin film samples.

To prepare the undoped crystals, pure C_{60} powder was first extracted from carbon soot via standard liquid chromatography with an alumina column. The powder was baked at 250°C under dynamic vacuum for 24 hours and then sealed in quartz tubes with a few hundred torr of argon gas. Sealed tubes were placed in a gradient furnace with the powder held at 650°C; crystals formed in the tube at about 450°C. With this vapor transport method, crystals with flat, shiny faces up to a few millimeters across could be obtained in a few days. X-ray diffraction studies confirmed the fcc (face-centered-cubic) crystal structure and lattice constant reported previously (*4*) for solid C_{60}.

Electrical contacts to the samples were made prior to doping by first evaporating silver onto the crystal surfaces and then attaching gold wires with conducting silver paint. Both Van der Pauw (*5*) and in line four-probe geometries were employed (with similar results). The mounted samples were then sealed together with fresh potassium metal in a Pyrex glass apparatus with tungsten feedthrough leads. Uniform doping was accomplished using a repetitive high-temperature dope-anneal cycle. First, both the sample and dopant were heated uniformly in a furnace while the sample resistance was continuously monitored. The temperature was raised from room temperature to about 200°C at a rate of 6°C per minute. At about 150°C, the resistance of the sample dropped down to within the measurable range of the ohm meter (20 mΩ); thereafter the resistivity of the sample dropped continually to a few hundred mΩ-cm within a few minutes. The tube was maintained at about 200°C for approximately one-half hour until the resistance of the sample reached a minimum. At this point the potassium end of the tube was cooled to room temperature and the sample alone was annealed at about 200° to 250°C overnight. Then the potassium end was reheated to ≈200°C and the sample was further doped until a lower resistivity minimum was reached. The sample alone was then again annealed for several hours. This doping and annealing process was repeated until the resistance reached an equilibrium state. For transport measurements the sample cell was injected with a helium exchange gas to ensure good thermal conduction, and a diode temperature sensor was mounted in the cell adjacent to the crystal.

The dc electrical resistivity ρ was measured versus temperature for a crystal of K_3C_{60} (Fig. 1). Crystals from different preparation batches yielded similar results. Near room temperature the resistivity is about 5 mΩ-cm, comparable to that obtained for K_3C_{60} films at room temperature (*1*, *3*). However, because of geometrical uncertainties associated with the contact pads, the absolute value of the resistivity should be considered reliable only to within a factor of 2. Below room temperature, $\rho(T)$ falls in a metal-like fashion with distinct curvature. At T_c the resistivity drops abruptly to zero, with a transition width < 200 mK. The inset in Fig. 1 shows $\rho(T)$ near T_c in detail. The temperature has been swept slowly (~50 mK per minute) near the transition temperature showing no difference in T_c between cooling and warming.

The $\rho(T)$ behavior shown in Fig. 1 for the single crystal is in contrast to $\rho(T)$ observed by other groups for potassium-

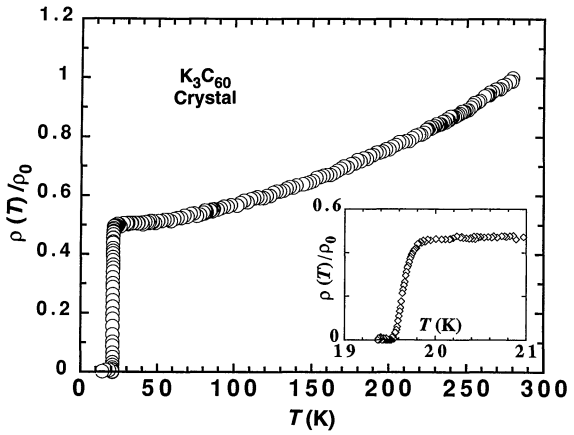

Fig. 1. Normalized dc electrical resistivity $\rho(T)$ for single-crystal K_3C_{60}. The ρ_0 is the resistivity at T = 280 K. The inset shows the $\rho(T)$ behavior near the superconducting transition temperature T_c = 19.8 K.

Department of Physics, University of California at Berkeley, and Materials Sciences Division, Lawrence Berkeley Laboratory, Berkeley, CA 94720.

*To whom correspondence should be addressed.